Available online at www.sciencedirect.com
ScienceDirect
Inorganica Chimica Acta 362 (2009) 887–893
Inorganica Chimica Acta
www.elsevier.com/locate/ica

Synthesis and characterization of platinum(II) complexes of 2N1O-donor ligands with a pendent indole ring

Yuichi Shimazaki [a,*], Tatsuo Yajima [b], Yasuo Nakabayashi [b], Yoshinori Naruta [a], Osamu Yamauchi [b,*]

[a] *Institute for Materials Chemistry and Engineering, Kyushu University, Higashi-ku, Fukuoka 812-8581, Japan*
[b] *Unit of Chemistry, Faculty of Engineering, Kansai University, Suita, Osaka 564-8680, Japan*

Received 3 December 2007; received in revised form 29 January 2008; accepted 31 January 2008
Available online 9 February 2008

This paper is dedicated to Professor Dr. Bernhard Lippert in celebration of his outstanding contribution to chemistry and with the very best wishes for his future activities

Abstract

The Pt(II) complexes of 2N1O-donor ligands containing a pendent indole, 3-[*N*-2-pyridylmethyl-*N*-2-hydroxy-3,5-di(*tert*-butyl)benzylamino]ethylindole (Htbu-iepp), and 1-methyl-3-[*N*-2-pyridylmethyl-*N*-2-hydroxy-3,5-di(*tert*-butyl)benzylamino]ethylindole (Htbu-miepp) (H denotes an ionizable hydrogen), were synthesized, and the structure of [Pt(tbu-iepp)Cl] (**1**) was determined by X-ray analysis. Complex **1** prepared in CH_3CN was revealed to have the C2 atom of the indole ring bound to Pt(II) with the Pt(II)–C2 distance of 1.981(3) Å. On the other hand, [Pt(tbu-miepp)Cl] (**2**) was concluded to have a phenolate coordination instead of the C2 atom of the indole ring by ^{1}H NMR spectra. Reaction of **1** with 1 equiv. of Ce(IV) in DMF gave the corresponding one-electron oxidized species, which exhibited an ESR signal at $g = 2.004$ and an absorption peak at 567 nm, indicating the formation of the Pt(II)–indole-π-cation radical species. The half-life, $t_{1/2}$, of the radical species at −60 °C was calculated to be 43 s ($k_{obs} = 1.6 \times 10^{-2}$ s^{-1}).

Keywords: Pt(II) complexes; Indole; Cyclometalation; Indole-π-cation radical; Pt(II)–indole bond

1. Introduction

The indole group of the tryptophan (Trp) residue in proteins is known to form a hydrophobic environment for protein stabilization and specific binding of molecules [1–3] and to be involved in electron transfer pathways [4–6]. It is sometimes located close to the active center of metalloenzymes with π–π stacking interaction. In the active center of cytochrome *c* peroxidase, the indole rings of Trp 51 and Trp 191 were revealed to be stacked with the heme and the coordinated imidazole ring of histidine 175, respectively [7]. The indole ring of Trp 191 plays an important role in the catalytic cycle; one of the reaction intermediate, compound I, has been considered to be the ferryl heme and Trp 191 indole-radical cation [4–6]. Trp coordinates to metal ions through the amino and carboxylate groups and may undergo intramolecular stacking interactions [8–11] as seen in $[Cu(L)(Trp)]ClO_4$ (L = 2,2′-bipyridine [12] or 1,10-phenanthroline [13]), but the indole ring has not been known to be involved in metal binding in biological systems, although it can form various bonds with metals such as palladium in synthetic chemistry [14,15].

We reported earlier that the Cu(I) complexes of tripodal ligands having an indole moiety in place of one of the coordinating groups were found to have a Cu(I)–(C2=C3) η^2 bond in a tetrahedral structure [16]. Pd(II) reacts with indole-3-acetate (IA) in the 3*H*-indole form in the presence of pyridine (py) to give a dimeric complex, $[Pd_2(IA)_2(py)_2]$,

* Corresponding authors. Tel./fax: +81 72 855 8102 (O. Yamauchi).
E-mail addresses: yshima@ms.ifoc.kyushu-u.ac.jp (Y. Shimazaki), oyamauchi36bioin@wonder.ocn.ne.jp (O. Yamauchi).

0020-1693/$ - see front matter © 2008 Elsevier B.V. All rights reserved.
doi:10.1016/j.ica.2008.01.046

where Pd(II) binds with the deprotonated indole C3 atom and the carboxylate oxygen atom of IA to form a *spiro* ring and in addition with the imine nitrogen atom of the other Pd(II)-bound IA molecule [17]. Kostić et al. developed Pd(II) and Pt(II) complexes which function as unique artificial peptidases, which recognize the indole moiety and cleave the adjacent amide or peptide bond specifically [18–21]. Examples are also known for Pd(II)–indole C2 bonding as a result of a cyclopalladation-like reaction [22,23]. Recently, we reported some Pd(II) complexes of 2N1O donor ligands with a pendent indole moiety (Scheme 1), which were found to be interconvertible between the Pd(II)–phenolato(O) and Pd(II)–indole(C2) complexes with a 2N1O1Cl- and a 2N1C1Cl-donor set, respectively [24]. One-electron oxidation of the Pd(II)–indole(C2) complex yielded the corresponding Pd(II)–indole π-cation radical species. Further, the conversion to the Pd(II)–indole species was concluded to be dependent on the phenolate O-donor properties, the formation ratio of the indole-binding complex to the phenolate complex being higher for the complexes with a higher pK_a value of the phenol moiety [25]. However, the interconversion or the formation of the Pd(II)–indole σ-bonding was limited by factors such as the distance between the indole ring and the Pd center and the existence of the phenol moiety and the unsubstituted indole NH moiety (Scheme 1).

Very recently, we have reported that the properties of the group 10 metal complexes depend on the central metal ion [26], and especially their oxidation behavior and properties of oxidized species are very different. With these points in mind, we now studied the behavior of the pendent indole ring in the Pt(II) complexes of the same 2N1O-donor ligands used for the Pd(II) complexes involving a phenol, a pyridine, and a tertiary amine as metal binding sites (Fig. 1) [24]. The structure of a novel indole C2 binding Pt(II) complex and the formation of the indole π-cation radical species upon oxidation with cerium(IV) are reported.

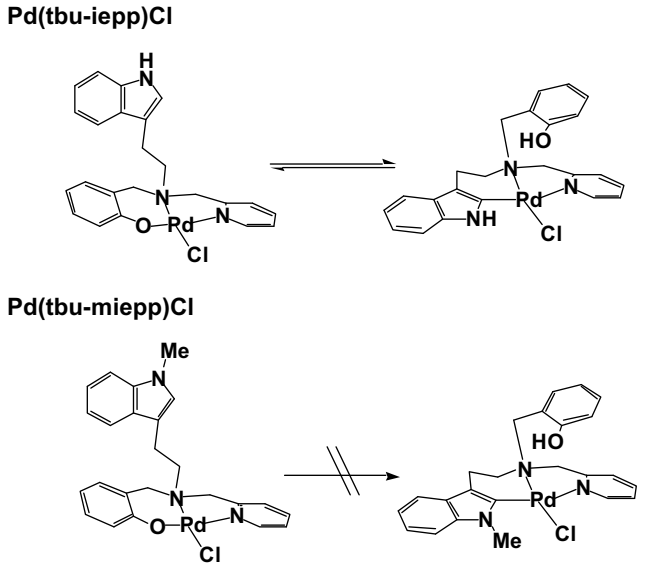

Scheme 1. Interconversion between phenolate and indole-binding Pd(II) complexes (*tert*-butyl groups are omitted for clarity).

2. Experimental

2.1. Materials and methods

K_2PtCl_4 and triethylamine were obtained from Wako, and other chemicals were obtained from Tokyo Kasei. All the chemicals used were of the highest grade available and were further purified whenever necessary [27]. Solvents were also purified before use by standard methods [27]. DMSO-d_6 was purchased from Cambridge Isotope Laboratory. Synthesis of [*N*-2-pyridylmethyl-*N*-2-hydroxy-3,5-di(*tert*-butyl)benzylamino]ethylindole (Htbu-iepp), 1-methyl-3-[*N*-2-pyridylmethyl-*N*-2-hydroxy-3,5-di(*tert*-butyl)benzylamino]ethylindole (Htbu-miepp), and [*N*-2-pyridylmethyl-*N*-2-hydroxy-3,5-di(*tert*-butyl)benzylamino]ethane (Htbu-etpp) have been reported previously [24,28]. Electronic spectra were measured with a Shimadzu UV-3101PC spectrophotometer. ^{1}H NMR measurements were performed with a JEOL JNM-GSX-400 (400 MHz) NMR spectrometer. Frozen solution ESR spectra were taken at 77 K in quartz tubes with 4-mm inner diameter on a JEOL JES-RE1X X-band spectrometer equipped with a standard low-temperature apparatus. The *g* values were calibrated with a Mn(II) marker used as a reference.

2.2. Synthesis of complexes

2.2.1. [Pt(tbu-iepp)Cl] (1)

To a suspension of Htbu-iepp (0.47 g, 1.0 mmol) in CH_3CN (20 mL) was added an aqueous solution of

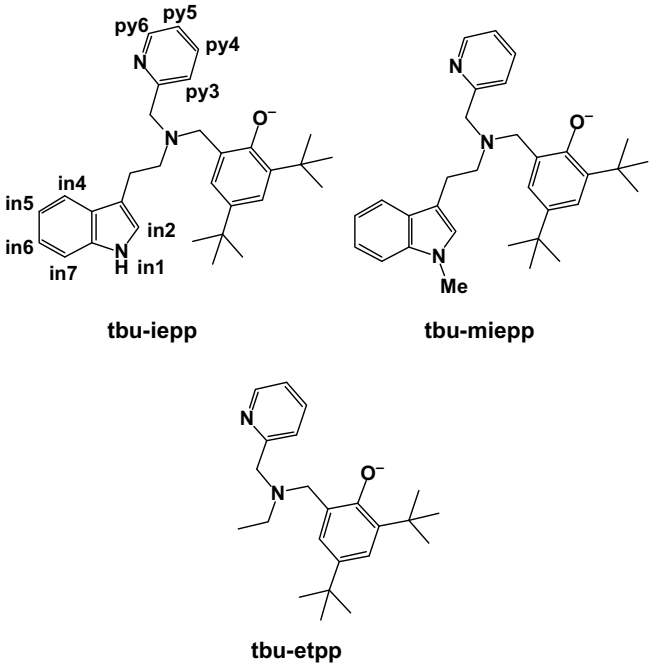

Fig. 1. Structures of ligands.

K_2PtCl_4 (0.42 g, 1.0 mmol), and the mixture was refluxed overnight. The solution was filtrated and kept standing at room temperature to give pale yellow crystals. *Anal*. Calc. for $C_{31}H_{38}N_3OClPt$ (**1**): C, 53.25; H, 5.48; N, 6.01. Found: C, 53.18; H, 5.41; N, 6.02%. ^{1}H NMR (400 MHz, DMSO-d_6): δ (vs TMS) 9.60 (s, 1H), 8.69 (d, 1H), 8.47 (s, 1H), 7.74 (d, 1H), 7.73 (t, 1H), 7.35 (q, 1H), 7.25 (q, 1H), 7.20 (m, 2H), 6.85 (m, 3H), 4.71 (d, 1H), 4.32 (d, 1H), 4.17 (d, 1H), 3.98 (q, 1H), 3.57 (m, 1H), 1.23 (s, 9H), 1.15 (s, 9H).

2.2.2. [Pt(tbu-miepp)Cl] (2) and [Pt(tbu-etpp)Cl] (3)

These complexes were prepared in a manner similar to that described for **1** as pale yellow solids. *Anal.* Calc. for $C_{32}H_{40}N_3OClPt$ (**2**): C, 53.89; H, 5.65; N, 5.89. Found: C, 53.85; H, 5.41; N, 5.88%. ^{1}H NMR (400 MHz, DMSO-d_6): δ (vs TMS) 9.00 (d, 1H), 8.18 (t, 1H), 7.77 (d, 1H), 7.47 (t, 1H), 7.25 (d, 1H), 7.12 (d, 1H), 7.08 (d, 1H), 7.02 (t, 1H), 6.88 (s, 1H), 6.75 (m, 2H), 4.96 (d, 1H), 4.72 (d, 1H) 4.64 (d, 1H), 4.32 (d, 1H), 3.59 (s, 3H), 2.90 (m, 3H), 2.61 (d, 1H), 1.36 (s, 9H), 1.20 (s, 9H). *Anal.* Calc. for $C_{23}H_{33}N_2OClPt$ (**3**): C, 47.30; H, 5.69; N, 4.80. Found: C, 47.25; H, 5.71; N, 4.78%. ^{1}H NMR (400 MHz, DMSO-d_6): δ (vs TMS) 9.00 (d, 1H), 8.17 (t, 1H), 7.74 (d, 1H), 7.47 (d, 1H), 7.06 (d, 1H), 6.93 (d, 1H), 4.71 (d, 1H) 4.54 (d, 1H), 4.48 (d, 1H), 4.06 (d, 1H), 2.58 (m, 2H), 1.35 (s, 9H), 1.21 (s, 9H), 0.88 (t, 3H).

2.3. X-ray structure determination

The X-ray experiments were carried out for a well-shaped single crystal of complex **1** on a Rigaku RAXIS imaging plate area detector with graphite monochromated Mo Kα radiation ($\lambda = 0.71073$ Å). The crystal was mounted on a glass fiber. To determine the cell constants and orientation matrix, three oscillation photographs were taken for each frame with the oscillation angle of 3° and the exposure time of 3 min. Intensity data were collected by taking oscillation photographs. Reflection data were corrected for both Lorentz and polarization effects. The structure was solved by the direct method and refined anisotropically for non-hydrogen atoms by full-matrix least-squares calculations. Each refinement was continued until all shifts were smaller than one-third of the standard deviations of the parameters involved. Atomic scattering factors were taken from the literature [29]. Except for the hydrogen atom of the phenol OH group, all hydrogen atoms were located at the calculated positions, assigned a fixed displacement, and constrained to ideal geometry with C–H = 0.95 Å and N–H = 0.90 Å. The thermal parameters of calculated hydrogen atoms were related to those of their parent atoms by $U(H) = 1.2U_{eq}(C,N)$. The hydrogen atom of the phenol OH group was located from the difference Fourier map. All the calculations were performed by using TEXSAN crystallographic software program package from Molecular Structure Corporation [30]. Summaries of the fundamental crystal data and experimental parameters for the structure determination of complex **1** are given in Table 1.

Table 1
Crystallographic data of complex **1**

	1
Formula	$PtC_{31}H_{38}N_3OCl$
Formula weight	610.51
Crystal color, habit	orange, platelet
Crystal dimensions (mm)	0.10 × 0.08 × 0.06
Crystal system	monoclinic
a (Å)	8.529(1)
b (Å)	15.251(3)
c (Å)	21.750(3)
β (°)	92.054(6)
V (Å^3)	2827.2(9)
Space group	$P2_1/n$
Z-value	4
D_{calc} (g/cm^3)	1.643
$F(000)$	1392.00
μ (Mo Kα) (cm^{-1})	50.86
$2\theta_{max}$ (°)	54.9
Observed reflections	46627
Independent reflections	6441
Reflections used	6441
Number of variables	334
R_1 [$I > 2\sigma(I)$][a]	0.018
R_w (all data)[b]	0.053

[a] $R_1 = \sum\|F_o| - |F_c\|/\sum|F_o|$ for $I > 2\sigma(I)$ data.
[b] $R_w = \{\sum\omega(|F_o| - |F_c|)^2/\sum\omega F_o^2\}^{1/2}$; $\omega = 1/\sigma^2(F_o) = \{\sigma_c^2(F_o) + p^2/4F_o^2\}^{-1}$.

3. Results and discussion

3.1. Preparation of Pt(II) complexes

2N1O-donor tripod-like ligands, Htbu-iepp, where H denotes an ionizable hydrogen, reacted with K_2PtCl_4 in 1:1 (v/v) CH_3CN/H_2O at 80 °C to give [Pt(tbu-iepp)Cl] (**1**) as pale yellow crystals. On the other hand, Htbu-miepp, which is inferred to have the same ligand structure as that of Htbu-iepp except the *N*-methylindole moiety, and Htbu-etpp, which has no indole moiety, reacted with K_2PtCl_4 under the same conditions to give [Pt(tbu-miepp)Cl] (**2**) and [Pt(tbu-etpp)Cl] (**3**) as a pale yellow powder, respectively. Elemental analysis of complexes **1**–**3** revealed that they have a deprotonated 2N1O-donor ligand and one chloride ion. Interestingly, while the corresponding Pd(II) complexes were obtained by the addition of a base such as triethylamine [24], it was not necessary for preparing these Pt(II) complexes. For the Pd(II) complexes the addition of a base assisted the conversion of the phenolate complexes to the indole-binding species [25]. However, such a conversion by base was not observed for any of the Pt(II) complexes, but instead the Pt(II)–ligand systems showed a color change to dark brown and gave some decomposition products, which were not studied any further.

3.2. Crystal structure of [Pt(tbu-iepp)Cl] (1)

X-ray crystal structure analysis revealed that **1** was a cyclometalation species having a mononuclear square-planar geometry formed by the indole C2 carbon, an amine

nitrogen, a pyridine nitrogen, and a chloride ion, as shown in Fig. 2. The Pt–C2 bond length is 1.981(3) Å (Table 2), which is within the normal range of the Pd–C2 distances for the indole-binding Pd(II) complexes of the ligand series and the Pt–C2 distances for the indole-binding Pt(II) complexes [23,24] but is slightly shorter than the values for the Pt–C bonds of Pt-phenyl complexes [31–33]. However, the Pt(II)–C2 distance in **1** is much shorter than the distances reported for the metal–indole complexes (Pd(II)–C3 = 2.12–2.15 Å [17]; Cu(I)–C2 and Cu(I)–C3 = 2.23–2.27 Å) [16]. The indole C2–C3 bond length in **1** (1.388(3) Å) is longer than that of the indole-binding Pd(II) and Cu(I) complexes and uncoordinated indole ring [16,17]. This may reflect a stronger effect of Pt(II) binding on the indole ring than that of Pd(II) and Cu(I) binding. The Pt–N bond lengths of **1** are 2.082(2) and 2.063(2) Å for Pt–N(pyridine) and Pt–N(amine) (Table 2), respectively, and the order of these bond lengths can be found for the other Pt complexes [32–34] and is in agreement with the observations with the Pd(II) complexes [24]. The phenol ring of **1** is located above the coordinated pyridine ring to be involved in the intramolecular π–π stacking, where the shortest C_{indole}–$C_{pyridine}$ distance is 3.177(4) Å and the angle between the average planes of the two aromatic rings is 34.3°. It is interesting to note in this connection that the side chain phenol ring stacks with the coordinated pyridine ring but not with the indole ring. Such a trend in stacking was also observed for the indole-binding and phenolate-binding Pd(II) complexes [24].

3.3. Characterization of Pt(II) complexes

The absorption spectra of **1** and **2** in DMF in the range 300–1000 nm showed a similar strong peak at 363 (ε = 7500) and 364 nm (ε = 6000), respectively. However, the ^{1}H NMR spectra of **1** and **2** in DMSO-d_6 were very different. The chemical shifts for **2** were very similar to those of [Pd(tbu-miepp)Cl], whose side chain indole ring is not stacked with the coordinated pyridine ring (Fig. 3 and Table 3) [24,25]. This result suggests that the structure of complex **2** is a phenolate complex and that the side chain indole ring is not coordinated to Pt(II). Further, the ^{1}H NMR chemical shifts for **2** were also very similar to those of **3** which is without a pendent aromatic ring, indicating that the side chain indole ring is not stacked with the coordinated pyridine ring in **2** (Scheme 2). On the other hand, large shift differences were observed for the pyridine and indole proton signals between **1** and **2** in DMSO (Fig. 4 and Table 3); the signals of pyridine C3 through C6 protons (py3–py6) in **1** shifted upfield relative to those of **2** with the chemical shift differences, $\Delta\delta = -(\delta_{complex1} - \delta_{complex2})$, of +0.2 to +0.6 ppm. The shifts of the indole signals ($\Delta\delta = -0.5$ to +0.1 ppm) observed for the Pt(II) complexes as well as the corresponding Pd(II) complexes are in contrast with the rather small differences observed between the Cu(I)-η^2-coordinated indole and free indole ($|\Delta\delta| = <0.1$ ppm) [16] and are ascribed to a stronger

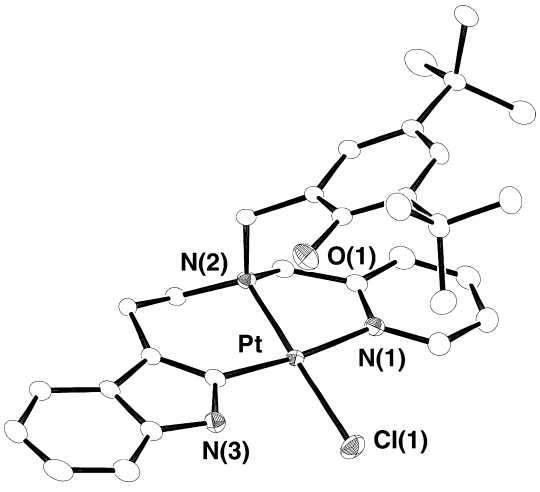

Fig. 2. ORTEP view of [Pt(tbu-iepp)Cl] (**1**) drawn with the thermal ellipsoids at 50% probability level and atomic labeling scheme.

Table 2
Selected bond lengths (Å) and angles (°) for **1**

	1
Bond lengths	
Pt–N(1)	2.082(2)
Pt–N(2)	2.063(2)
Pt–C(2)	1.981(3)
Pt–Cl	2.3125(7)
Bond angles	
N(1)–Pt–N(2)	82.75(8)
N(1)–Pt–C(2)	174.20(8)
N(1)–Pt–Cl	93.85(6)
N(2)–Pt–C(2)	91.55(9)
N(2)–Pt–Cl	176.32(6)
C(1)–Pt–Cl	91.88(7)

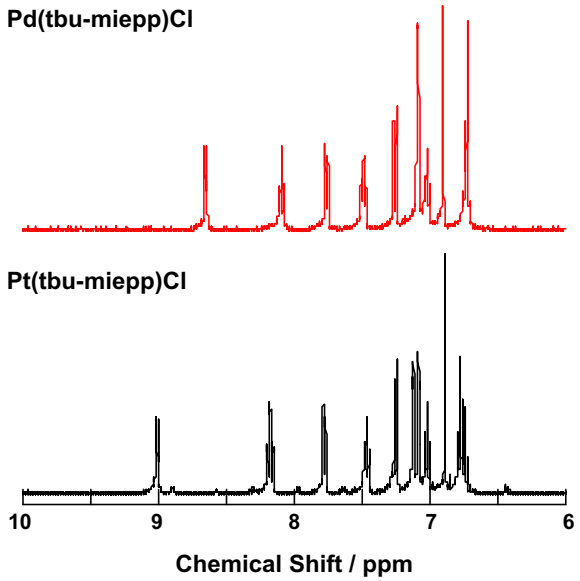

Fig. 3. ^{1}H NMR spectra of metal-tbu-miepp complexes (metal = Pd(II) and Pt(II)).

Table 3
^{1}H NMR chemical shifts (δ/ppm) and upfield shifts ($\Delta\delta$)[a] of pyridine and indole proton signals for Pd(II) complexes in DMSO-d_6

	δ ($\Delta\delta$) (ppm)		
	tbu-iepp (**1**)	tbu-miepp (**2**)	tbu-etpp (**3**)
py3	7.20 (+0.57)	7.77	7.74 (+0.03)
py4	7.73 (+0.45)	8.18	8.17 (+0.01)
py5	7.20 (+0.27)	7.47	7.47 (0)
py6	8.69 (+0.31)	9.00	9.00 (0)
in1	8.47		
in2		6.88	
in4	7.35 (−0.10)	7.25	
in5	6.85 (−0.10)	6.75	
in6	6.85 (+0.17)	7.02	
in7	7.25 (−0.50)	6.75	

[a] $\Delta\delta = -(\delta - \delta_{complex2})$, where $\delta_{complex2}$ refers to the shift for **2**.

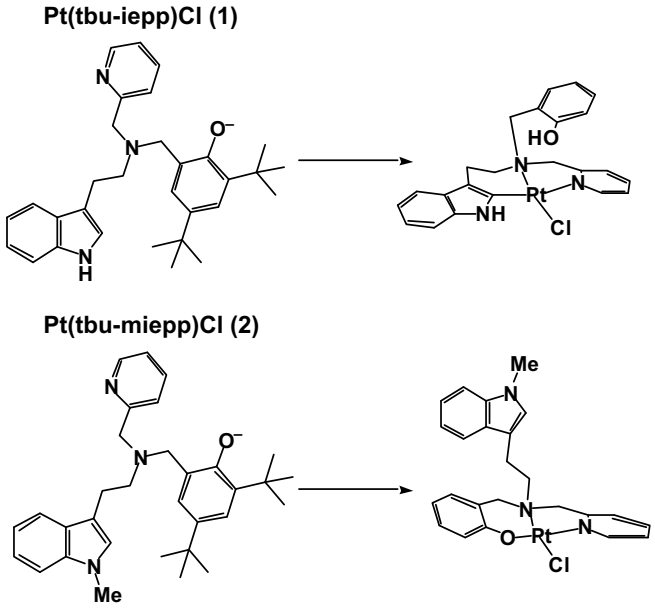

Scheme 2. Formation of the Pt complexes with N2O ligands containing an indole ring (*tert*-butyl groups in complexes are omitted for clarity).

σ-donation to Pt(II) and Pd(II) than to Cu(I) by the indole ring. These observations support that similar side chain conformations and coordination structures are maintained both in the solid state and in solution. The indole-binding Pt(II) complex **1** is very stable in DMSO at room temperature; the ^{1}H NMR spectrum of **1** in DMSO showed no spectral changes over one week, whereas the corresponding Pd(II) complex, [Pd(tbu-iepp)Cl], in DMSO was found to undergo interconversion between the indole-binding species and the phenolate complex [24,25]. The difference in behavior in solution may be in line with the general properties of the Pd and Pt complexes in ligand exchange reactions [35].

3.4. Oxidation with Ce(IV)

Oxidation of **1** by one equivalent of Ce(IV) in DMF at −60 °C caused a color change from yellow to green, giving

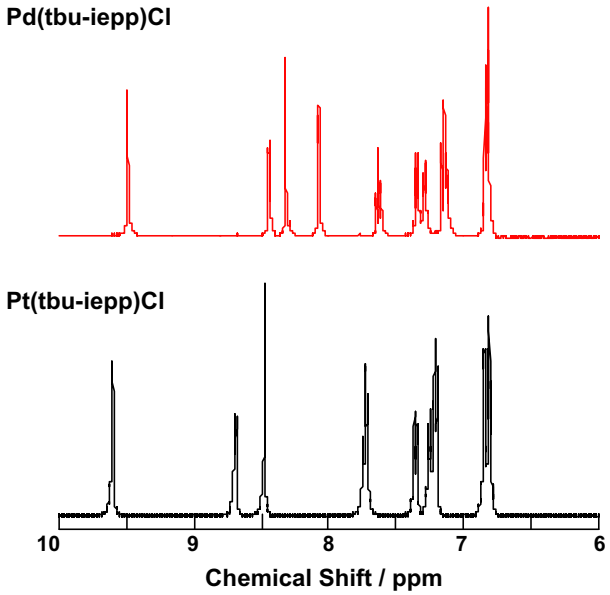

Fig. 4. ^{1}H NMR spectra of indole-binding metal-tbu-iepp complexes (metal = Pd(II) and Pt(II)).

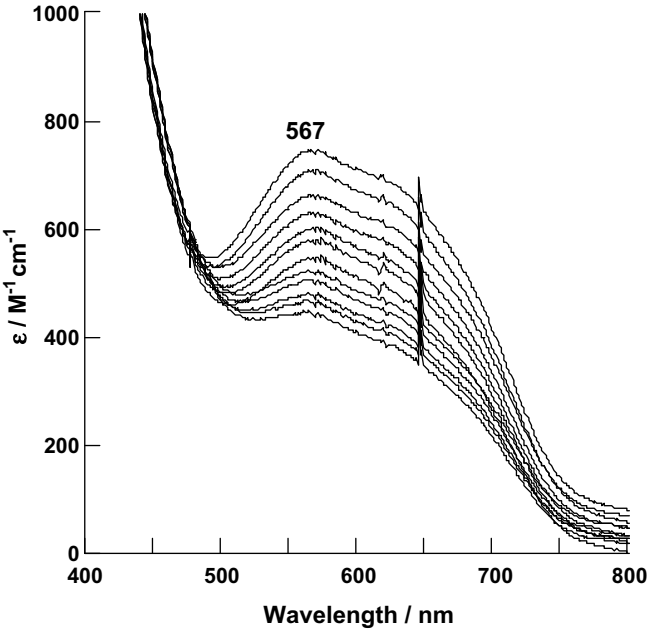

Fig. 5. Absorption spectral changes of oxidized **1** with time in DMF at −60 °C (5.0×10^{-4} M). The spectra were recorded at 10-s intervals.

a new peak at 567 nm in the visible absorption spectrum (Fig. 5). The reaction was found to be a one-electron oxidation process from the reaction stoichiometry. The ESR spectrum of oxidized **1** exhibited a new sharp signal at $g = 2.004$, and the amount of unpaired electron was calculated to be more than 0.85 from the integrated spectrum (Fig. 6). On the other hand, the absorption spectra of **2** and **3** remained unchanged upon the addition of Ce(IV), and no peaks characteristic of the phenoxyl radical were observed in our previous studies [26,36–39]. The indole radicals from tryptophan

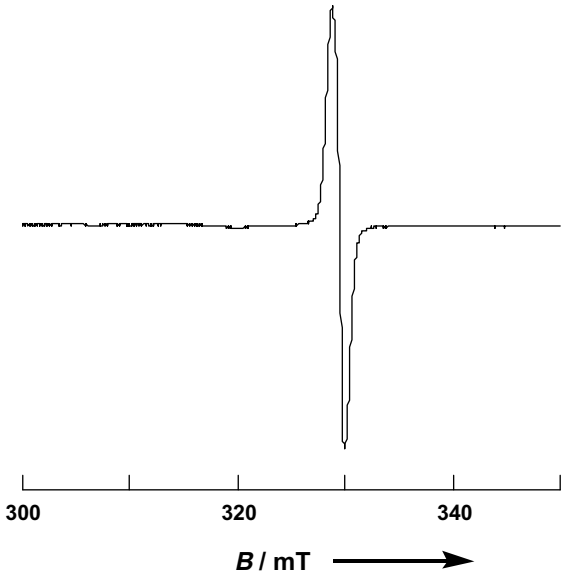

Fig. 6. ESR spectrum of one-electron oxidized **1** in DMF at 77 K. Concentration, 5.0×10^{-4} M; microwave power, 1 mW; modulation amplitude, 0.63 mT.

and *N*-methylindole have been reported to show a characteristic absorption band in the region 510–560 nm [6,40,41], where the indole-π-cation radical and the neutral indolyl radical give a band centered at 560 and 510 nm, respectively. The oxidized Pd(II) complex having the same ligand, [Pd(tbu-iepp)Cl], showed a similar absorption peak at ~550 nm, which has been assigned to the Pd(II)–indole-π-cation radical species. On the basis of these considerations, we assign the oxidized form of **1** having a peak at 567 nm to the indole π-cation radical species, although the assignment of the shoulder appearing at 600–650 nm is not clear at present. The unpaired electron is inferred to be localized in the indole ring. When the green solution of oxidized **1** in DMF was left to stand at −60 °C, it rapidly turned yellow, and the 567-nm absorption peak disappeared in the first-order decay. The half-life, $t_{1/2}$, of oxidized **1** was calculated to be 43 s ($k_{obs} = 1.6 \times 10^{-2}\ s^{-1}$). This result shows that the oxidized form of **1** was slightly more stable than that of [Pd(tbu-iepp)Cl] ($t_{1/2} = 20$ s, $k_{obs} = 3.5 \times 10^{-2}\ s^{-1}$), indicating that the Pt(II) ion has a weak stabilizing effect on the indole-radical [24]. This characteristic may be due to the inertness of Pt(II) in ligand exchange. Further stabilization of the indole-radical species may be attained by introducing protecting groups into the indole ring. It should be mentioned in this connection that, when a methyl group was introduced into the NH moiety of the indole ring as the *N*-alkylindole of tub-miepp in **2**, no Pt(II)–indole bond was formed.

4. Concluding remarks

We prepared and characterized the Pt(II) complexes of a series of tripod-like 2N1O-donor ligands with a phenol ring and a pendent indole moiety. The direct indole carbon–Pt(II) bonding has been established by the molecular structure of **1**, which was also concluded for the solution of **1** in DMSO-d_6 by the downfield shifts of the indole protons due to effective σ-donation by the C2 atom. However, interconversion between the Pt–indole and Pt–phenolate complex was not detected, which is probably due to the inert character of Pt(II) in ligand exchange reactions. One-electron chemical oxidation of the Pt(II)–indole complex, **1**, yielded the corresponding Pt(II)–indole-π-cation radical species, which is supported by the characteristic 567-nm absorption peak and the ESR signal of the radical species. The stability of the indole-π-cation radical species was slightly higher than that from the corresponding Pd(II) complex, which may also arise from the inertness of Pt(II).

The present observations will add to our knowledge of the versatile nature of the indole ring in the metal coordination sphere and give clues to its functions in a variety of systems.

Acknowledgements

We gratefully acknowledge the support of this work by the Grants-in-Aid for Scientific Research (No. 17750055 to Y.S. and No. 16350036 to O.Y.) from the Ministry of Education, Culture, Sports, Science and Technology of Japan.

Appendix A. Supplementary material

CCDC 669313 contains the supplementary crystallographic data for complex **1**. These data can be obtained free of charge from The Cambridge Crystallographic Data Centre via www.ccdc.cam.ac.uk/data_request/cif. Supplementary data associated with this article can be found, in the online version, at doi:10.1016/j.ica.2008.01.046.

References

[1] S.K. Burley, G.A. Petsko, Science 229 (1985) 23.
[2] S.K. Burley, G.A. Petsko, Adv. Protein Chem. 39 (1988) 125.
[3] E.A. Meyer, R.K. Castellano, F. Diederich, Angew. Chem. Int. Ed. 42 (2003) 1210.
[4] S.S. Isied, Met. Ions Biol. Syst. 27 (1991) 1.
[5] J.M. Nocek, J.S. Zhou, S. De Forest, S. Priyadarshy, D.N. Beratan, J.N. Onuchic, B.M. Hoffman, Chem. Rev. 86 (1996) 2359.
[6] J. Stubbe, W.A. van der Donk, Chem. Rev. 98 (1998) 705.
[7] T.L. Poulos, R.E. Fenna, Met. Ions Biol. Syst. 30 (1994) 25.
[8] B.E. Fischer, H. Sigel, J. Am. Chem. Soc. 102 (1980) 2998.
[9] G. Liang, H. Sigel, Z. Naturforsch. 44B (1989) 1555.
[10] O. Yamauchi, A. Odani, J. Am. Chem. Soc. 107 (1985) 5938.
[11] O. Yamauchi, A. Odani, M. Takani, J. Chem. Soc., Dalton Trans, (2002) 3411, and references cited therein.
[12] H. Masuda, T. Sugimori, A. Odani, O. Yamauchi, Inorg. Chim. Acta 180 (1991) 73.
[13] K. Aoki, H. Yamazaki, J. Chem. Soc., Dalton Trans. (1987) 2017.
[14] B.S. Lane, M.A. Brown, D. Sames, J. Am. Chem. Soc. 127 (2005) 8050.
[15] S. Cacchi, G. Fabrizi, Chem. Rev. 105 (2005) 2873.
[16] Y. Shimazaki, H. Yokoyama, O. Yamauchi, Angew. Chem. Int. Ed. 38 (1999) 2401.
[17] M. Takani, H. Masuda, O. Yamauchi, Inorg. Chim. Acta 235 (1995) 367.

[18] N.V. Kaminskaia, T.W. Johnson, N.M. Kostić, J. Am. Chem. Soc. 121 (1999) 8663.
[19] N.V. Kaminskaia, G.M. Ullmann, D.B. Fulton, N.M. Kostić, Inorg. Chem. 39 (2000) 5004.
[20] N.V. Kaminskaia, N.M. Kostić, Inorg. Chem. 40 (2001) 2368.
[21] N.M. Milović, N.M. Kostić, Met. Ions Biol. Syst. 38 (2001) 145.
[22] M. Nonoyama, K. Nakajima, Polyhedron 18 (1998) 533.
[23] G. Cravotto, F. Demartin, G. Palmisano, A. Penoni, T. Radice, S. Tollari, J. Organomet. Chem. 690 (2005) 2017.
[24] T. Motoyama, Y. Shimazaki, T. Yajima, Y. Nakabayashi, Y. Naruta, O. Yamauchi, J. Am. Chem. Soc. 126 (2004) 7378.
[25] Y. Shimazaki, M. Tashiro, T. Motoyama, S. Iwatsuki, T. Yajima, Y. Nakabayashi, Y. Naruta, O. Yamauchi, Inorg. Chem. 44 (2005) 6044.
[26] Y. Shimazaki, T. Yajima, F. Tani, S. Karasawa, K. Fukui, Y. Naruta, O. Yamauchi, J. Am. Chem. Soc. 129 (2007) 2559.
[27] D.D. Perrin, W.L.F. Armarego, D.R. Perrin, Purification of Laboratory Chemicals, Pergamon Press, Elmsford, 1966.
[28] T. Yajima, Y. Shimazaki, N. Ishigami, A. Odani, O. Yamauchi, Inorg. Chim. Acta 337 (2002) 193.
[29] J.A. Ibers, W.C. Hamilton, International Tables for X-ray Crystallography, vol. IV, Kynoch, Birmingham, 1974.
[30] Crystal Structure Analysis Package, Molecular Structure Corporation, 1985/1999.
[31] B.R. James, in: G. Wilkinson, F.G.A. Stone, E.W. Abel (Eds.), Comprehensive Organometallic Chemistry, Pergamon Press, Oxford, 1982 (Chapter 51).
[32] A. Clein, E.J.L. McInnes, W. Kaim, J. Chem. Soc., Dalton Trans. (2002) 2371.
[33] M.R. Plutino, L.M. Scolaro, A. Albinati, R. Romeo, J. Am. Chem. Soc. 126 (2004) 6470.
[34] F.H. Allen, Acta Crystallogr. B 58 (2002) 380.
[35] C.T.J. Barnard, M.J.H. Russel, in: G. Wilkinson, R.D. Gillard, J.A. McCleverty (Eds.), Comprehensive Coordination Chemistry, vol. 5, Pergamon, Oxford, 1987 (Chapter 53).
[36] Y. Shimazaki, S. Huth, S. Hirota, O. Yamauchi, Bull. Chem. Soc. Jpn. 73 (2000) 1187.
[37] Y. Shimazaki, S. Huth, S. Odani, O. Yamauchi, Angew. Chem. Int. Ed. 39 (2000) 1666.
[38] Y. Shimazaki, S. Huth, S. Karasawa, S. Hirota, Y. Naruta, O. Yamauchi, Inorg. Chem. 43 (2004) 7816.
[39] Y. Shimazaki, R. Kabe, S. Huth, F. Tani, Y. Naruta, O. Yamauchi, Inorg. Chem. 46 (2007) 6083.
[40] M.R. DeFelippis, C.P. Murthy, F. Broitman, D. Weinraub, M. Faraggi, M.H. Klapper, J. Phys. Chem. 95 (1991) 3416.
[41] S. Solar, N. Getoff, P.S. Surdhar, D.A. Armstrong, A. Singh, J. Phys. Chem. 95 (1991) 3639.